

**Table 1 : Difference and agreement between US2AI and Cart for different measurements**

Variables	Mean difference $\pm$ SD	Limits of Agreement	Range
LV Ejection Fraction	-2.446 $\pm$ 3.527	-9.359; 4.466	13.825
LA Volume Indexed	2.421 $\pm$ 3.291	-4.030; 8.872	12.902
E/A ratio	-0.005 $\pm$ 0.123	-0.245; 0.235	0.480
E/e' Mean	0.206 $\pm$ 1.031	-1.814; 2.226	4.040
Tricuspid Regurgitation Vmax	0.275 $\pm$ 0.44	-0.587; 1.137	1.724
LA Reservoir Strain	-1.250 $\pm$ 4.024	-9.137; 6.637	15.774

#### P10-02

##### Natural Wave Velocity as a Marker of Fibrosis in a Reversible Right Ventricular Pressure Overload Model

Maelys Venet<sup>1</sup>, Matteo Ponzone<sup>2</sup>, Josh Gaupol<sup>2</sup>, Aimen Malik<sup>2</sup>, Jerome Baranger<sup>3</sup>, Mark K. Friedberg<sup>4</sup>, Jason T. Maynes<sup>2</sup>, John G. Coles<sup>2</sup>, Olivier Villemain<sup>1</sup>. <sup>1</sup>CHU de Bordeaux, Pessac, France; <sup>2</sup>The Hospital for Sick Children, Toronto, ON, Canada; <sup>3</sup>Physics for Medicine, Paris, France

**Background:** Right ventricular (RV) pressure overload, commonly observed in conditions such as tetralogy of Fallot or pulmonary hypertension drives adverse RV remodeling. Identifying irreversible remodeling processes and determining optimal timing for therapeutic interventions remain critical clinical challenges in congenital heart diseases. This study aimed to assess natural wave velocity (NWV) as a marker of RV myocardial stiffness in a rat model of RV pressure overload and to explore its potential for reversibility following pressure unloading. **Methods:** Twenty rats underwent PAB, and six sham-operated rats served as controls. After 3 weeks, half of the PAB rats were debanded to simulate pressure unloading, while the other half remained banded until 6 weeks. Conventional echocardiography and ultrafast ultrasound were performed preoperatively, early post operatively, at 3 weeks and at 6 weeks. All animals underwent terminal analysis at 6 weeks with histological analysis. **Results:** NWV increased shortly after PAB and continued to rise with sustained pressure overload. Following PAB reversal, NWV remained elevated despite normalization of conventional echocardiographic morphological and functional parameters. Notably,

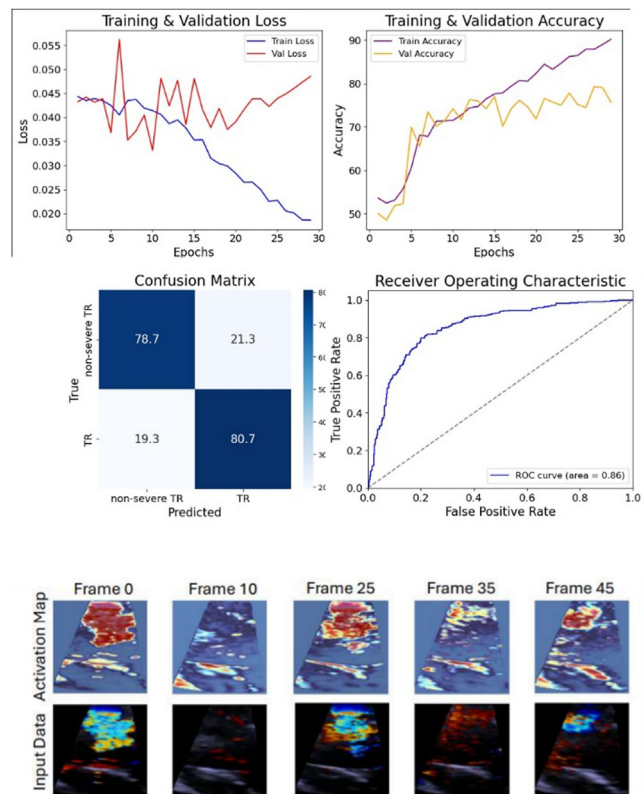
NWV stopped increasing after debanding, whereas it continued to rise in the kept banded group. A strong correlation was observed between RV NWV and histological fibrosis content ( $R=0.78$ ,  $p<0.001$ ). **Conclusion:** NWV outperformed other functional and morphological parameters in detecting fibrosis-related changes in pressure-overload conditions. Early identification of elevated NWV may guide timely interventions, potentially preventing irreversible RV damage and optimizing patient outcomes.

#### P10-03

##### An AI Model to Distinguish Moderate From Severe Tricuspid Regurgitation

Anthony Wu, Purnima Gurung, Amanda Warren, Donna Kim, Shady Mikhail, Jin Kyung Kim, Xiaohui Xie, Peter Chang, Jennifer Xu. University of California, Irvine, Orange, CA

**Background:** Severe tricuspid regurgitation (TR) is associated with a one-year mortality rate of 36%, yet over 90% of patients are not referred for intervention due to prohibitive surgical risk. While percutaneous TR interventions show promise, their mortality benefit remains unproven. Accurate grading of TR on transthoracic echocardiography (TTE) is challenging and may lead to underestimation of severity. This study aimed to develop an AI model to differentiate moderate from severe TR. **Methods:** A total of 3,604 TTE clips from 1,201 patients (severe TR: 1,680 clips; moderate TR: 1,924 clips) were labeled. A multiple instance learning AI model was trained using spatial and temporal convolutional feature extraction blocks, with data from 961 patients used for training and 240 for validation. A perceptron model classified instances as severe or moderate TR, with predictions aggregated via mean pooling. Model performance was assessed using sensitivity, specificity, and area under the receiver operating characteristic curve (AUROC). **Results:** The AI model demonstrated strong discriminatory ability with an AUROC of 0.86, a sensitivity of 79%, and a specificity of 81% (Figure 1). Spatial activation mapping confirmed its ability to identify structural and Doppler flow abnormalities in TR (Figure 2). **Conclusion:** Our AI model accurately differentiates between moderate and severe TR, providing a novel framework to improve TR assessment and optimize patient selection for emerging percutaneous therapies.



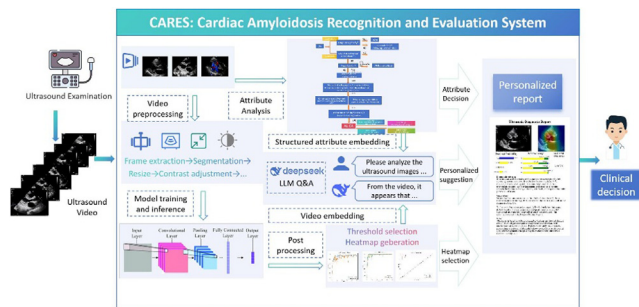
#### P10-04

##### Echoing Recovery: Systematic Review and Meta-Analysis on Sonothrombolysis in ST-Segment Elevation Myocardial Infarction Treated With Primary Percutaneous Coronary Intervention

Akshat Banga<sup>1</sup>, Sidharth Misra<sup>2</sup>, Lakshmi Sai Niharika Janga<sup>1</sup>, Xiaonan Ying<sup>1</sup>, Maheen Erum<sup>3</sup>, Angelo Caputi<sup>4</sup>, Vikas Bansal<sup>5</sup>, Saurbha Dani<sup>6</sup>, Karupiah Arunachalam<sup>7</sup>, Andrew Goldsweig<sup>8</sup>. <sup>1</sup>Mount Auburn Hospital, Harvard Medical School, Cambridge, MA; <sup>2</sup>Armed Forces Medical College, Pune, India; <sup>3</sup>Lady Hardinge Medical College, New Delhi, India; <sup>4</sup>Cook County Hospital, Chicago, IL; <sup>5</sup>WellSpan Health, York, PA; <sup>6</sup>Lahey Hospital & Medical Center, Burlington, MA; <sup>7</sup>Orlando Health, Orlando, FL; <sup>8</sup>Baystate Medical Center, Springfield, MA

**Background:** Despite advancements in STEMI management, microvascular dysfunction after PCI remains a critical barrier to optimal myocardial recovery. Sonothrombolysis

failure. It is essential to establish an early and efficient diagnostic framework for patients suspected of AL-CA, to guide therapeutic and prognostic decision-making. **Methods:** This study established an artificial intelligence-driven framework—Cardiac Amyloidosis Recognition and Evaluation System (CARES)—integrating echocardiographic imaging data with clinical multimodal variables to enable automated diagnosis and prognostic evaluation of AL-CA. Additionally, large language model (LLM) was applied to generate personalized clinical reports. CARES achieved adaptive focusing on characteristic features through feature analysis of input images. Model performance was validated in real-world diagnostic outcomes. **Results:** Our study included 1001 patients ( $55.0 \pm 15.7$  y, male (65.1%)) diagnosed with left ventricular hypertrophy (LVH) in database from three medical sub-centers. Cases were classified into 3 subgroups: hypertrophic cardiomyopathy (HCM) group ( $n=172$ , male (69.2%)), AL-CA group ( $n=53$ , male (54.1%)), LVH group ( $n=758$ , male (61.8%)). The five-fold cross-validated receiver operating characteristic (ROC) curves showed favorable results (AL-CA (AUC:  $0.98 \pm 0.02$ ), HCM (AUC:  $0.96 \pm 0.02$ ), LVH (AUC:  $0.95 \pm 0.01$ )), indicating high diagnostic accuracy. **Conclusions:** Our research established an AI-assisted multimodal reporting system, where a vision-based deep neural network extracts discriminative features from echocardiographic images, compensating for variability in operator-dependent interpretations, while clinical data are integrated into a diagnostic decision tree. CARES presents the first integration of a deep learning framework for automated assessment of echogenicity of AL-CA. The innovative integration of LLMs further enables automated generation of patient-specific reports, integrating strain analysis and quantitative biomarkers. CARES, as the non-invasive diagnosis framework of AL-CA, holds significant clinical value in therapeutic evaluation and risk stratification.



PC1-21

### Ultrasound-Driven MSC-NV Nanomotors for Precision Targeting and Repair of Injured Myocardium

Jinhong Liu, Jianfeng Chen, Haobo Yang, Sirui Tian, Haichao Yang, Jiaxu Wang, Jiaxin Shan, Xinwen Hu, Shouqiang Li, Zhuo Wang, Xiaoping Leng. The 2nd affiliated hospital of Harbin Medical University, Harbin, China

**Background:** Myocardial infarction (MI) remains a leading cause of morbidity and mortality worldwide, with current clinical treatments failing to achieve effective myocardial repair. Mesenchymal stem cell-derived nanovesicles (MSC-NVs) have shown promise in promoting cardiac regeneration as an alternative to MSCs. However, their therapeutic efficacy is hindered by circulation dynamics and biological barriers, limiting efficient delivery. Our previous studies demonstrated that ultrasound-driven nanomotors could achieve high-efficiency targeted delivery. In this study, we aimed to develop MSC-NV nanomotors integrating multi-targeted therapy with ultrasound-driven motion to achieve precise myocardial repair. **Methods:** Asymmetric modification of MSC-derived nanovesicles was achieved using iron oxide nanoparticles (IONP), resulting in the MSC-NV nanomotor (IONP-NV). A custom-built ultrasound propulsion system was employed to modulate frequency and amplitude for controlled nanomotor movement. Following the establishment of a murine MI model, tail vein injections were administered, and ultrasound propulsion was applied. In vivo imaging was utilized to assess nanomotor targeting of ischemic myocardium, while M-mode echocardiography was performed to evaluate cardiac function recovery across different treatment groups. **Results:** The MSC-NV nanomotors were successfully synthesized and characterized. Multiple characterization techniques confirmed the successful asymmetric modification with IONPs, facilitating efficient propulsion. In vitro experiments demonstrated controlled motion of nanomotors. Without ultrasound, they exhibited Brownian motion. Upon ultrasound activation, they moved in a directed manner, reaching a maximum velocity of  $12 \mu\text{m/s}$ . They also retained motility in blood environments. In the MI mouse model, ultrasound-driven nanomotors exhibited enhanced cardiac accumulation and superior cardiac function recovery compared to non-propelled counterparts. **Conclusion:** Our study presents a promising strategy that integrates the therapeutic potential of stem cell-derived nanovesicles with ultrasound-driven nanomotors, enabling precise targeting and repair of injured myocardium.

PC1-22

### Echocardiography and Artificial Intelligence in the Cardiac Amyloidosis Referral Pathway

Ashley P. Akerman<sup>1</sup>, Will Hawkes<sup>1</sup>, Jeremy A. Slivnick<sup>2</sup>, Gary Woodward<sup>1</sup>, Christopher G. Scott<sup>3</sup>, Mathew S. Maurer<sup>4</sup>, Sarah Cuddy<sup>5</sup>, Jordan B. Strom<sup>6</sup>, Jamie O'Driscoll<sup>7</sup>, Roberto M. Lang<sup>2</sup>, Patricia A. Pellikka<sup>3</sup>, Ross Upton<sup>1</sup>. <sup>1</sup>Ultrasonics Ltd, Oxford, United Kingdom; <sup>2</sup>University of Chicago, Chicago, IL; <sup>3</sup>Mayo Clinic, Rochester, MN; <sup>4</sup>Columbia University, New York, NY; <sup>5</sup>Brigham and Women's Hospital, Boston, MA; <sup>6</sup>Beth Israel Deaconess Medical Center, Boston, MA; <sup>7</sup>University of Leicester, Leicester, United Kingdom

**Background:** Echocardiography is critical in identification of patients at risk of cardiac amyloidosis (CA). Low cost and high accessibility ensure that patients can be screened in

high volumes, and appropriately referred for confirmatory testing, monitoring, and treatment. This study aimed to examine how echocardiography and artificial intelligence (AI) may be utilized in the CA diagnostic pathway. **Methods:** Retrospective, multi-site data comprising 4255 patients without CA, and 560 patients with CA was collected for external validation of an AI model for identification of CA (AI-CA; EchoGo Amyloidosis). Clinical utility (decision curve analysis) was modelled under assumptions of lower (1%) and higher (6%) prevalence to refer patients for confirmatory testing. Referral decisions were based on echocardiographic red flags for CA, increased wall thickness or AI-indicated presence of heart failure (AI-HF; EchoGo Heart Failure), plus a positive AI-CA report. **Results:** Patients from 17 clinical sites were  $60 \pm 20$  y,  $26.8 \pm 6.3 \text{ kg/m}^2$ , with high prevalence of comorbidities, including increased wall thickness (33%) and positive AI-HF (30%). Patients with CA comprised light chain (34%) and transthyretin CA (variant and wild type, 13% and 53%, respectively). Figure 1 illustrates the proportion of patients with CA correctly referred (standardized net benefit; top), and number of referrals avoided without missing a patient with CA (net reduction in interventions; bottom), for low (left) and high prevalence settings (right). In low prevalences, and corresponding low threshold for referring a patient (1-3%), utilizing either red flag and a positive AI-CA report resulted in 11-64% (range dependent on threshold probability) more patients with CA being correctly referred compared to either red flag alone, and 11-21% reduction in the number of referrals without missing any CA patients. In higher prevalence settings, and correspondingly higher thresholds (6-10%), an extra 11-33% of CA patients, and 11-18% fewer referrals were observed. There was little difference in the choice of red flag trigger prior to AI-CA (~1%). **Conclusions:** Utilizing echocardiographic red flags for CA in combination with a positive report from an AI model to refer patients for CA has demonstrated clinical utility in low- and high-prevalence settings.

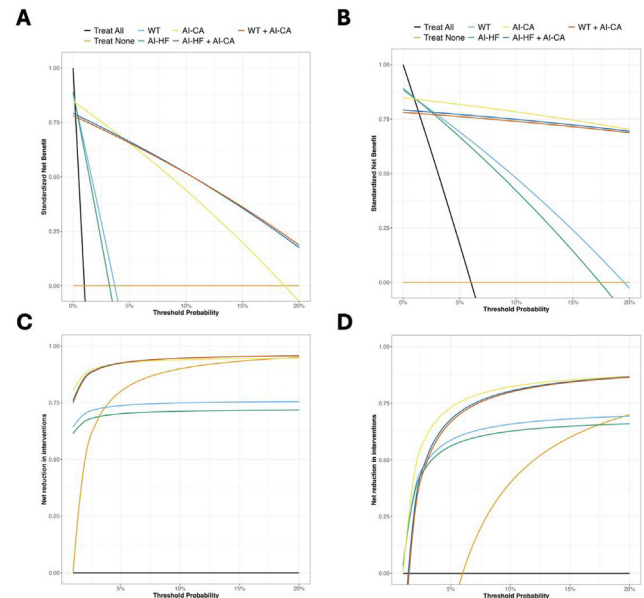


**Figure 1.** Decision curve analysis modelling referral for confirmatory cardiac amyloidosis (CA) testing based on echocardiographic red flags for CA and artificial intelligence. Increased wall thickness on echocardiography ("WT"; PWT or IVS  $\geq 12 \text{ mm}$ ) or AI-indicated presence of heart failure ("AI-HF"; EchoGo Heart Failure) was compared with the joint probabilities of a red flag and positive report for AI-indicated presence of CA ("AI-CA"; EchoGo Amyloidosis). Decisions to refer all ("Treat All") and refer none ("Treat None") are provided as clinical benchmarks.

PC1-23

### Aortic Stenosis Severity Classification: A Diagnostic Quandary with an Artificial Intelligence Solution

Hema Krishna<sup>1,2</sup>, Wouter Ouwerkerk<sup>3,4</sup>, Joshua H. Arnold<sup>1</sup>, Siddharth Bhayani<sup>1</sup>, Matthew Frost<sup>5</sup>, Zhuo Jiang<sup>5</sup>, Cyril Equilbec<sup>2</sup>, Carolyn SP Lam<sup>5,4,6</sup>, Patricia A. Pellikka<sup>7</sup>, Sanjiv Shah<sup>8</sup>, Dawood Darbar<sup>1,2</sup>, Mayank M. Kansal<sup>1,2</sup>. <sup>1</sup>University of Illinois at Chicago, Chicago, IL; <sup>2</sup>Jesse Brown Veterans Affairs Medical Center, Chicago, IL; <sup>3</sup>Amsterdam UMC, Amsterdam, Netherlands; <sup>4</sup>National Heart Centre Singapore, Singapore, Singapore; <sup>5</sup>Us2.ai, Singapore, Singapore; <sup>6</sup>Duke-NUS Medical School, Singapore, Singapore; <sup>7</sup>Mayo Clinic, Rochester, MN; <sup>8</sup>Northwestern University, Bluhm Cardiovascular Institute, Chicago, IL

**Background:** Aortic stenosis (AS) is serious valve disease diagnosed by echocardiography. Guidelines produce discordant classification and diagnostic uncertainty in half of AS patients, often due to low-flow (stroke volume index  $\leq 35 \text{ mL/m}^2$ ). Here, we show two convolutional neural network (CNN)-augmented methods which grade AS severity and predict outcomes in a low-flow rich population. **Methods:** AS patients with echocardiograms performed 2005-2023 were included. Three classification methods were compared. Ground truth was taken as the cardiologist classification per the original report. Second, a deterministic algorithm based on peak aortic jet velocity (Vmax), mean transvalvular pressure gradient (MG), aortic valve area by the continuity equation, and dimensionless index was created, with CNN-performed measurements (Us2.ai, Singapore). Third, a gradient boosted model (GBM) was developed using CNN measurements against a ground truth of cardiologist classification. **Results:** The GBM was trained ( $n=537$ ), then validated ( $n=214$ ) on a cohort of 968 patients. MG, Vmax, and dimensionless index were the most salient